Spatial Dissociation of Subretinal Drusenoid Deposits and Impaired Scotopic and Mesopic Sensitivity in AMD

Yuhua Zhang,[1,2] SriniVas R. Sadda,[1,2] David Sarraf,[2,3] Thomas A. Swain,[4] Mark E. Clark,[4] Kenneth R. Sloan,[4] William E. Warriner,[4,5] Cynthia Owsley,[4] and Christine A. Curcio[4]

[1]Doheny Eye Institute, Los Angeles, California, United States
[2]Department of Ophthalmology, University of California - Los Angeles, Los Angeles, California, United States
[3]Jules Stein Eye Institute, Los Angeles, California, United States
[4]Department of Ophthalmology and Visual Sciences, University of Alabama at Birmingham, Birmingham, Alabama, United States
[5]Research Computing, University of Alabama at Birmingham, Birmingham, Alabama, United States

Correspondence: Yuhua Zhang, Doheny Eye Institute, Department of Ophthalmology, University of California - Los Angeles, 1355 San Pablo St, Los Angeles, CA 90033, USA;
yzhang@doheny.org.

CO and CAC contributed equally as senior authors.

Received: July 15, 2021
Accepted: February 3, 2022
Published: February 25, 2022

Citation: Zhang Y, Sadda SR, Sarraf D, et al. Spatial dissociation of subretinal drusenoid deposits and impaired scotopic and mesopic sensitivity in AMD. *Invest Ophthalmol Vis Sci.* 2022;63(2):32. https://doi.org/10.1167/iovs.63.2.32

Purpose. Subretinal drusenoid deposits (SDD) first appear in the rod-rich perifovea and can extend to the cone-rich fovea. To refine the spatial relationship of visual dysfunction with SDD burden, we determined the topography of mesopic and scotopic light sensitivity in participants with non-neovascular AMD with and without SDD.

Methods. Thirty-three subjects were classified into three groups: normal ($n = 9$), AMD–Drusen (with drusen and without SDD; $n = 12$), and AMD–SDD (predominantly SDD; $n = 12$). Mesopic and scotopic microperimetry were performed using 68 targets within the Early Treatment Diabetic Retinopathy Study grid, including points at 1.7° from the foveal center (rod:cone ratio, 0.35). Age-adjusted linear regression was used to compare mesopic and scotopic light sensitivities across groups.

Results. Across the entire Early Treatment Diabetic Retinopathy Study grid and within individual subfields, the three groups differed significantly for mesopic and scotopic light sensitivities (all $P < 0.05$). The AMD–SDD group exhibited significantly decreased mesopic and scotopic sensitivity versus both the normal and the AMD–Drusen groups (all $P < 0.05$), while AMD–Drusen and normal eyes did not significantly differ (all $P > 0.05$). The lowest relative sensitivities were recorded for scotopic light levels, especially in the central subfield, in the AMD–SDD group.

Conclusions. SDD-associated decrements in rod-mediated vision can be detected close to the foveola, and these deficits are proportionately worse than functional loss in the rod-rich perifovea. This finding suggests that factors other than the previously hypothesized direct cytotoxicity to photoreceptors and local transport barrier limitations may negatively impact vision. Larger prospective studies are required to confirm these observations.

Keywords: age-related macular degeneration, drusen, subretinal drusenoid deposit, mesopic sensitivity, scotopic sensitivity

AMD is a multifactorial disease of the photoreceptor support system causing vision loss.[1] Histopathologic[2–8] and functional[9–11] studies have shown that photoreceptor degeneration and functional deterioration is already underway in early and intermediate AMD, as a continuation of aging, and in relation to extracellular deposits on the apical and basal side of RPE, namely, drusen and subretinal drusenoid deposit (SDD). Dysregulation of a system of outer retinal lipid homeostasis for cone- and rod-specific physiology is proposed to underlie formation of drusen and SDD, respectively, because of their differential cholesterol content and distinctive topography.[5,6] Soft drusen are prevalent in the central macula, where the density (cells per millimeters squared of the retinal surface) of cones and Müller glia is high.[12,13] In contrast, SDD appear first near the vascular arcades in the superior retina, where rod density is high in an elliptical ring.[5,14,15] With time, SDD may extend to the cone-rich fovea.[16]

We previously speculated that, similar to drusen, SDD impose a transport barrier between photoreceptors and the choroidal circulation and exert direct cytotoxicity, because the deposits contact the cells.[5] Thus, one might predict that visual dysfunction would colocalize with the SDD load and distribution, with worse visual function far from the fovea (in perifovea) than near the fovea. Among the current methods of assessing rod and cone sensitivity at multiple locations in eyes with AMD and normal eyes, fundus-controlled microperimetry offers advantages including a spatially resolved grid of targets for visual sensitivity using fixation tracking, and the capacity for programmable disease-specific test patterns.[17]

Existing data show that eyes with AMD with SDD have markedly worse visual function than those lacking SDD.[18–32] Data also suggest that both steady-state sensitivity mediated by rods and rod-mediated dark adaption (RMDA), a

Investigative Ophthalmology & Visual Science

dynamic measure of retinoid resupply from the circulation, is spatially dissociated from the retinal location of SDD. Along the primary vertical retinal meridian, Fraser et al.[24] found that dark adaptation kinetics were most delayed within 6° of the foveal center. Flynn et al.[25] reported greatly decreased scotopic sensitivity and slowed or absent dark adaptation across the macula with the largest deficits close to the fovea in eyes with SDD. In cross-sectional and longitudinal studies, Tan et al.[28,30] observed that both rod-mediated sensitivity and RMDA were most impaired at a 4° eccentricity. Other studies, using the Early Treatment Diabetic Retinopathy Study (ETDRS) grid, show SDD eyes also have worse mesopic sensitivity in the outer ring than the central subfield.[18,19] Sensitivity was decreased similarly across the grid in eyes with drusen.[19]

In this study, we used microperimetry to assess light sensitivity in participants having non-neovascular AMD with and without SDD. We included test points close to the foveola (1.7°) where rods are sparse,[12] yet mesopic and scotopic sensitivities are measurable. Close-in points were included to allow mechanistic interpretations of outcomes relative to previous literature on topography of aging and AMD changes.[2,3,33] In particular, rod loss in aging and structural changes in outer retinal reflective bands associated with delayed RMDA are proportionately larger at distances from the foveal center of 0.5 mm (1.7°) than at greater eccentricities (2 mm, 6.8°).[2,34] In turn, we relate these findings to the foveal centration of processes leading to Bruch's membrane lipidization.[34]

Methods

The study followed the tenets of the Declaration of Helsinki, complied with the Health Insurance Portability and Accountability Act of 1996, and was approved by the Institutional Review Boards at the University of Alabama at Birmingham and the University of California – Los Angeles. Written informed consent was obtained from participants.

Subjects

Study participants with AMD were recruited from the clinical research registry of the Department of Ophthalmology and Visual Sciences of the University of Alabama at Birmingham and through its Retina Service. One author (Y.Z.) identified the subjects from the medical records of participants who had been diagnosed with AMD and with a best-corrected visual acuity (BCVA) of 20/100 or better to increase the likelihood of successful microperimetric testing. Subjects with neovascular AMD, center-involving geographic atrophy, diabetes, glaucoma, a history of retinal vascular occlusions, hereditary retinal dystrophy, and any vision-impairing ocular condition other than non-neovascular AMD were excluded. Enrollment did not impose a specific age criterion if prospective participants had an AMD diagnosis. Age-similar subjects with normal retinal examinations were recruited from the same registry. The inclusion criteria for normal subjects were age greater than 50 years old, no history of ocular and systemic disease, and BCVA of 20/40 or better. Refractive errors determined from the medical record were within ±6 diopters spherical and ±3 diopters cylinder for all participants.

Visual Acuity Test and Multimodal Imaging

The BCVA was measured on each eye separately using the Age-related Eye Disease Study (AREDS) refraction protocol and an electronic visual acuity computerized testing device, which has been validated against the ETDRS chart. Both eyes of the participant were dilated with 1% tropicamide and 2.5% phenylephrine. Multimodal clinical images were acquired from both eyes. Stereo color fundus photography was taken with a fundus camera (Zeiss 450 plus, Carl Zeiss Meditec Inc., Dublin, CA) with the Escalon digital system, using the three-field protocol of the AREDS study.[35] En face near infrared, blue reflectance, and fundus autofluorescence images were acquired using a confocal scanning laser ophthalmoscope (Spectralis, Heidelberg Engineering, Carlsbad, CA). Spectral domain optical coherence tomography (OCT) was acquired with the Spectralis instrument using a dense macular cube protocol (20° × 20° field of view, 121 B-scans, ART = 10) and enhanced depth imaging mode allowing for assessing the choroidal structure.

AMD Presence and Subject Categorization

Color fundus photographs were graded by a masked grader (author M.E.C.) trained by the University of Wisconsin Reading Center, using the AREDS nine-step severity scale for AMD.[35] Participants deemed to be in normal macular health met the criteria for AREDS grade 1 in both eyes.

Eyes were classified into three groups: normal, including subjects with normal macular examination; AMD–Drusen, including participants diagnosed with non-neovascular AMD with predominantly drusen and no SDD; and an AMD–SDD group, including participants with AMD with predominantly SDD.

The criterion for AMD–SDD was patterned lesions consistent with SDD detected with at least two imaging modalities, as follows[36]: yellow–white dots or ribbons (color fundus photography); hyper-reflective lesions (blue reflectance); hyporeflective or hyper-reflective spots or ribbons (near-infrared); or hypoautofluorescent lesions against a background of mildly elevated fundus autofluorescence. On OCT eyes with SDD displayed five or more definite hyperreflective mounds above the RPE in at least one B-scan.[37] By OCT, drusen were defined as focal or mound-shape deposits located posterior to the RPE + basal lamina band and anterior to the inner collagenous layer of Bruch's membrane.[38]

Before microperimetry testing, one author (Y.Z.) classified the eyes into groups so that the proper filter setting could be used in microperimetry (detailed elsewhere in this article). Later, these classifications were verified independently by two masked senior retina specialists (S.R.S., D.S.).

Mesopic and Scotopic Microperimetry

Mesopic and scotopic light sensitivity were measured in one eye from each subject using a microperimeter (MP1-S, Nidek USA Inc., San Jose, CA). This instrument can adjust for fixation during testing and allows positioning of targets over selected fundus areas by the operator. A near-infrared image of the fundus captured by the Spectralis OCT can be exported into the MP1-S for target-retinal image registration.

The manufacturer's setting of the MP1-S has a narrow dynamic range for testing light sensitivity (2 log units or 20 dB). Like others, we noted ceiling effects for the normal and AMD–Drusen groups and floor effects for the AMD–SDD

Investigative Ophthalmology & Visual Science

Table 1. Mesopic and Scotopic Microperimetry Settings

	Mesopic Test			Scotopic Test		
MP1-S Setting	**Normal**	**AMD–Drusen**	**AMD–SDD**	**Normal**	**AMD–Drusen**	**AMD–SDD**
Stimulus color	White	White	White	Blue	Blue	*Blue*
Stimulus size	Goldmann III	Goldmann III	Goldmann III	Goldmann III	Goldmann III	Goldmann III
Threshold strategy	4-2	4-2	4-2	4-2	4-2	4-2
Maximum stimulus intensity (cd/m^2)	12.7	12.7	12.7	0.255[17]	0.255[17]	2.550
Minimum stimulus intensity (background) (cd/m^2)	0.127	0.127	1.27	0.003[17]	0.003	0.026
Filters	NDA* (10 dB)	NDA (10 dB)	None	NDA (20 dB), short-pass (502 nm)	NDA (20 dB), short-pass (502 nm)	NDA (10 dB), short-pass (502 nm)

NDA, neutral density attenuation filter.

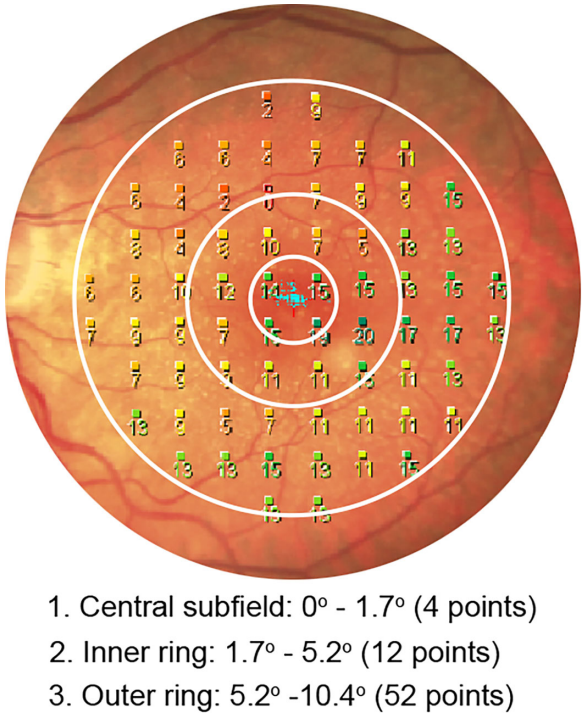

Figure 1. Macular light sensitivity was assessed in subfields of the ETDRS grid. Shown are the central subfield, inner ring, and outer ring of this grid, with the 68 test points indicated. Mean values for rods/mm^2, cones/mm^2, and rod:cone ratio at subfield test points, as determined by histology in older eyes with normal maculae,[2] are 15,787, 49,042, and 0.35 for the four points in the central subfield, 49,663, 19,563, and 2.7 for 12 points in the inner ring, and 79,895, 12,054, and 6.9 for 52 points in the outer ring, respectively.

group.[39,40] In particular, the ceiling effects may yield testing results that cannot differentiate between normal and AMD–Drusen patients. Therefore, we used different combinations of neutral density attenuation filters and a short-pass blue filter (502 nm) to expand the dynamic range to 3 log units (30 dB) (Table 1).

Both mesopic and scotopic sensitivities were measured at 68 test points using a Goldman size III target (0.43° or 118 µm) in the central 10.4° radius of the macula (Fig. 1). The light stimulus was presented for 200 ms using a 4-2 threshold strategy. We began with mesopic testing, which is generally easier to complete than scotopic testing. The subjects were light-adapted in normal room light for approximately 15 minutes. A 2° wide four-cross pattern in red color, was used as a fixation target. After a break, the patient underwent dark adaptation for 40 minutes in a dark room. Scotopic microperimetry was then conducted in the dark using the same 4-2 threshold strategy on the same target locations as used for mesopic testing, with a 2° wide four-cross pattern in white color as a fixation target. Mesopic and scotopic testing each took on average 15 minutes. Participants who had not been tested in the MP1-S within the prior 6 months underwent a practice pretest. To shield patients from stray light during adaptation and testing, heavy dark fabric was positioned around the instrument.

Data Analysis and Presentation

Topography of Light Sensitivity. For insight into how SDD affects vision, we agnostically tested sensitivity at many retinal locations to capture the different distributions of deposits and photoreceptors, and assigned 68 test points to subfields of the ETDRS grid. This grid is comprised of the central subfield (0°–1.7° radius), inner ring (1.7°–5.2° radius) and outer ring (5.2°–10.4° radius) (Fig. 1). Nominal values for photoreceptor densities and rod:cone ratio for test points in each subfield were determined from photoreceptor densities previously measured in flat-mounted tissues of older adults with normal maculae (Fig. 1).[2] Mean values for rods/mm^2, cones/mm^2, and rod:cone ratio are shown in the caption to Figure 1. Although the central subfield contains the fovea, the test points are near the edge of the subfield and stimulate both rods and cones. Actual values in individual tested patients will differ from these histological measurements, owing to age- and AMD-related cell loss and the stimulation of adjacent retinal areas. Nevertheless, these values allow inferences about the photoreceptor populations stimulated at the test points.

Subject Classification Agreement. Two experienced retinal specialists (S.R.S. and D.S.) reviewed all subjects' images independently, categorized eyes into three groups, and reconciled any differences. This consensus diagnosis was compared with the categorization used for participant testing (discussed elsewhere in this article) with Cohen's kappa statistic.

Statistical Analysis

Age was compared across groups using one-way ANOVA. Visual acuity (expressed in logMAR) was compared across groups using the Kruskal–Wallis test. Gender was compared across groups using Fisher's exact test. Measured light sensitivities were expressed as median and quartiles. Owing to

Investigative Ophthalmology & Visual Science

group differences in age (see Results), mesopic and scotopic sensitivities were compared among the three groups with age-adjusted linear regression. Light sensitivities in different subfields of the macula were compared within groups using the Wilcoxon signed-rank test. A two-sided P value of less than 0.05 was considered statistically significant. All statistical analyses were performed using SAS version 9.4 (SAS Institute, Cary, NC).

Graphical Presentation

The median sensitivities for each of the three groups was represented as a standard left eye[41] and displayed using custom MATLAB software (MathWorks, Natick, MA). Median sensitivities in decibels were plotted using a color scale designed for accurate data representation and accessibility by color-deficient readers.[42] Median light sensitivities and interquartile range were plotted with SAS version 9.4.

Results

A total of 33 eyes of 33 subjects were studied in 3 groups, normal (n = 9), AMD–Drusen (n = 12), and AMD–SDD (n = 12). Participant classification by two experienced retinal specialists and the initial classification used for participant testing showed excellent agreement (kappa = 0.90; 95% confidence interval, 0.78–1.0). Figure 2 shows representative cases demonstrating a typical distribution of AMD deposits, that is, abundant drusen in the central subfield and abundant SDD in the perifovea and sparing the fovea.

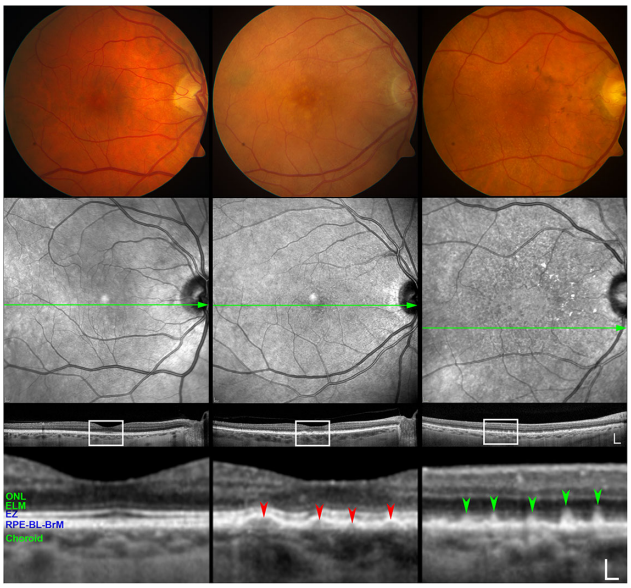

Figure 2. Representative multimodal retinal images of subjects in three diagnostic groups. Left column, eye in the normal group; middle column, eye in the AMD–Drusen group; right column, eye in the AMD–SDD group. Deposit distribution is typical of AMD cases, i.e., abundant drusen in the central subfield (middle column) and abundant SDD in the perifovea and sparing the fovea (right column). Top row, color fundus photograph; second row, near infrared (NIR) reflectance image. Green arrow lines indicate where spectral domain (SD) OCT were taken. Third row, SD-OCT B-scan taken along the corresponding green arrow line in NIR image; bottom row, magnified (×5) SD-OCT image within the white box in corresponding SD-OCT B-scan. Red arrowheads highlight four drusen. Green arrowheads highlight five SDD. ONL, outer nuclear layer; ELM, external limiting membrane; EZ, ellipsoid zone; RPE–BL–BrM, retinal pigment epithelium–basal lamina–Bruch's membrane. Scale bars in SD-OCT: 200 µm.

Normal participants were 65.2 ± 10.7 years old (range, 52–83 years) and AMD–Drusen participants were 69.3 ± 5.0 years old (range, 58–80 years). AMD–SDD participants were 76.7 ± 7.4 years old (range, 61–90 years) and thus significantly older than the other groups (P = 0.0064). The three groups exhibited similar BCVA (P = 0.2829), expressed in LogMAR as median (lower quartile, upper quartile): 0.00 (0.00, 0.00) for normal; 0.1 (0.00, 0.15) for AMD–Drusen; and 0.20 (−0.05, 0.30) for AMD–SDD. The corresponding Snellen equivalents as median (lower quartile, upper quartile) were 20/20 (20/20, 20/20) for normal, 20/25 (20/20, 20/32) for AMD–Drusen, and 20/32 (20/18, 20/40) for AMD–SDD. The groups had a similar gender distribution (P = 0.2736). Except for one Asian subject in the normal group, subjects were non-Hispanic White.

Among the 12 eyes in the AMD–drusen group, 11 eyes (AREDS 5–8) displayed multiple large soft drusen (>350 µm diameter) in the ETDRS central subfield, and 1 eye (AREDS grade 4) displayed central soft drusen of approximately 80 µm diameter. Among the 12 eyes in the AMD–SDD group, all exhibited SDD sparing the fovea, and 2 also showed soft drusen (approximately 300 µm diameter) in the central subfield. By considering SDD as "reticular drusen,"[43] 11 subjects in the AMD–SDD group were classified as an AREDS grade 5 to 8. One eye displayed noncentral geographic atrophy (approximately 500 µm in diameter, superior nasal 9° from the foveal center), and thus was assigned an AREDS grade 9.

After age adjustment with linear regression, there were significant differences among the three groups for mesopic and scotopic light sensitivities in the overall ETDRS grid and in all subfields (all $P < 0.05$) (Table 2). As shown in Figures 3 and 4 and Table 2, the AMD–SDD group exhibited significantly lower sensitivities compared with the normal and AMD–Drusen groups (all $P < 0.05$). The normal and AMD–Drusen groups did not significantly differ (all $P > 0.05$).

A graphical display of sensitivity (Fig. 3) showed that the lowest sensitivities were recorded for scotopic light levels, especially in the central subfield. Regional relationships were explored further by plotting median and quartile mesopic and scotopic sensitivities for the three groups in each of the ETDRS subfields, along with results of statistical comparisons, in Figure 4. This graph shows the overall lower sensitivity of eyes in the AMD–SDD group, under both testing conditions. Figure 4 also shows that poor sensitivity in the AMD–SDD group was apparent in the central subfield for mesopic ($P < 0.0339$) and especially scotopic ($P < 0.0001$) sensitivities. The normal and AMD–Drusen groups were similar at the two light levels and three subfields (the six conditions in Fig. 4).

A comparison of regions within individuals is shown in Tables 2 and 3. The most consistent difference found was lower scotopic sensitivity in central subfield vs. outer ring, for all three groups. Table 2 shows that median mesopic sensitivity was 3 to 5 dB lower in the central subfield in the AMD–SDD group relative to either AMD–drusen or normal groups (15 vs. 18 and 21 dB, respectively). Scotopic sensitivity was 10 to 12 dB lower in the central subfield in the AMD–SDD group relative to either AMD–Drusen or normal groups (0.9 vs. 11 and 12, respectively).

To compare the ETDRS rings from central to outer, the decibel scale of the light sensitivity was converted to light

Investigative Ophthalmology & Visual Science

Table 2. Mesopic and Scotopic Sensitivity (Median (Lower Quartile, Upper Quartile))

Visual Function	Number of Eyes	Overall ETDRS Grid (dB)	Central Subfield (dB)	Inner Ring (dB)	Outer Ring (dB)
Mesopic sensitivity					
Normal macular health	6	23.59 (22.11, 24.43)	20.88 (20.00, 23.25)	24.25 (23.42, 25.25)	23.64 (21.98, 24.29)
AMD–Drusen	12	21.29 (21.13, 23.46)	18.25 (16.00, 20.75)	22.50 (21.58, 24.92)	21.71 (21.08, 23.46)
AMD–SDD	12	15.43 (14.88, 16.73)	15.25 (11.50, 15.88)	16.83 (14.38, 17.92)	15.62 (14.50, 16.61)
P value*		<0.0001	0.0451	0.0025	<0.0001
Scotopic sensitivity					
Normal macular health	9	17.81 (17.59, 18.75)	12.25 (11.50, 13.25)	18.08 (17.17, 18.58)	18.10 (17.88, 19.35)
AMD–Drusen	12	16.63 (14.62, 18.29)	11.00 (10.38,12.38))	16.33 (14.04, 17.96)	17.04 (14.88, 18.96)
AMD–SDD	12	6.95 (4.68, 9.71)	0.88 (0.00, 2.00)	5.21 (2.75, 8.71)	7.98 (5.54, 10.33)
P value*		<0.0001	<0.0001	<0.0001	<0.0001

* All *P* values have been adjusted for age.

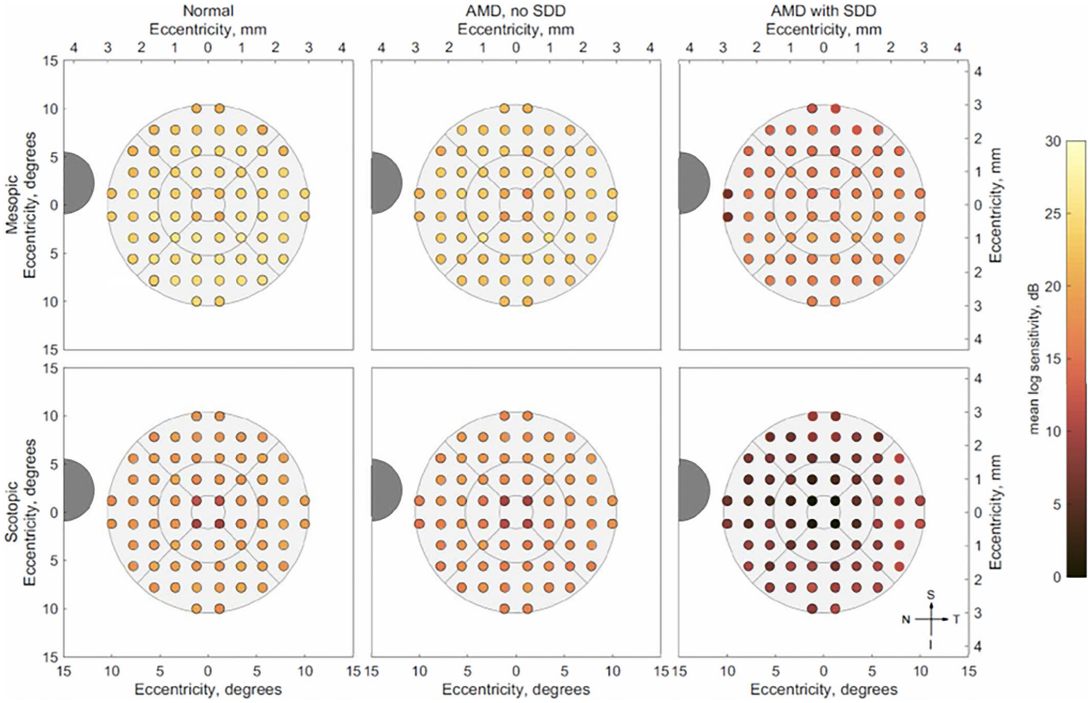

Figure 3. Map of median mesopic and scotopic light sensitivity measured in the three subject groups. Each dot indicates the 68 microperimetry target locations, within the subfields of the ETDRS. As evidenced by the shift to dark colors, the lowest sensitivities were recorded for AMD–SDD at both mesopic and scotopic light levels. Further within the scotopic maps, the lowest sensitivities were recorded within the central subfield.

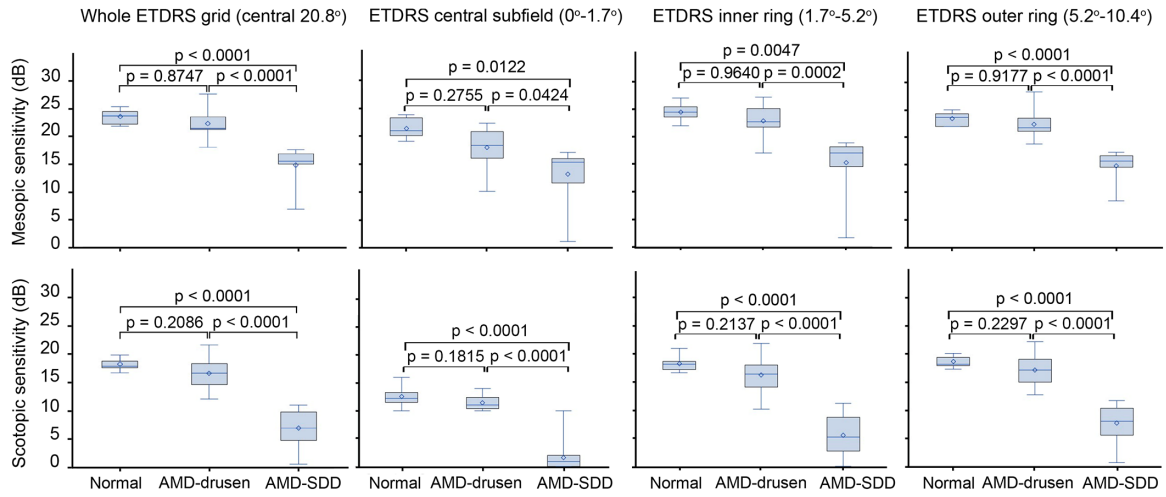

Figure 4. Sensitivity in the AMD–SDD group is worse than eyes in the AMD–Drusen, even in the central subfield, where rods are sparse. All *P* values were obtained from pairwise comparisons between subjects in different groups and were adjusted for age.

Investigative Ophthalmology & Visual Science

Table 3. Visual Field Sensitivities Compared by Retinal Region Within Groups

	Normal		AMD–Drusen		AMD–SDD	
Subfield	**Mesopic**	**Scotopic**	**Mesopic**	**Scotopic**	**Mesopic**	**Scotopic**
Central subfield vs. outer ring (*P* values)	0.0313	0.0039	0.0039	0.0005	0.0923	0.0005
Inner ring vs. outer ring (*P* values)	0.0625	0.2031	0.6523	0.0093	0.2036	0.0010

levels in units of cd/m^2 (Supplementary Table S1). The mesopic thresholds were elevated by 3.64-, 5.50-, and 6.33-fold in the AMD–SDD group compared with the corresponding areas in the normal group, while scotopic thresholds were elevated by 13.87-, 19.25-, and 10.25-fold (Supplementary Table S2). The outer and inner rings exhibited the largest relative elevation of mesopic and scotopic threshold, respectively. However, the light sensitivity is normally low in the central subfield compared with that in the inner and outer rings (1 vs. 0.46 vs. 0.53 for mesopic, 1 vs. 0.27 vs. 0.27 for scotopic threshold) (Supplementary Table S3). Considering this fact, we normalized the thresholds in different fields to the central subfield of the normal group (Supplementary Table S3). Mesopic thresholds in ETDRS rings from central to outer in the AMD–SDD group were elevated by 3.64-, 2.54-, and 3.35-fold, that is, a consistent difference. In contrast, scotopic thresholds were elevated by 13.87-, 5.13-, and 2.73-fold from the central to the outer. The central subfield contains the origin of the retinal and visual coordinate system, that is, the foveal center where visual acuity is the highest. Thus, normalizing the light sensitivity thresholds in different subfields to the central subfield of the normal subjects can justly disclose the impact of drusen and SDD on the light sensitivity in areas with different densities of cones and rods. The results show that the effective elevation of the threshold is proportionally much larger for scotopic sensitivity than mesopic in the central subfield for the AMD–SDD group.

It is possible that poor scotopic vision in AMD–SDD eyes may be due to the inclusion of patients with soft drusen in the ETDRS central subfield or other severe disease. Therefore, the two subjects with central soft drusen and the one with non-central geographic atrophy were removed from the SDD group. Differences when comparing the three groups for mesopic sensitivity in the central ETDRS subfield became insignificant ($P = 0.0578$); however, all other differences for scotopic light sensitivities remained significant ($P < 0.05$).

Discussion

Microperimetry precisely assesses mesopic and scotopic sensitivity over a fine spatial scale and in a standardized sampling pattern. Our study extends previous work by measuring mesopic and scotopic sensitivity in participants with non-neovascular AMD, with and without SDD, versus subjects with normal macular health per AREDS grading, using test points close to the foveola. Our study confirms previous reports of poor sensitivity in eyes with SDD in comparison with eyes without SDD,[18–32] even in the ETDRS central subfield where rods are sparse.[12] Observed sensitivities are low even without the direct presence of SDD in that location.[5,16] As detailed elsewhere in this article, our data show that scotopic vision is more severely affected than mesopic vision, and rod-mediated vision loss in general is worse near the fovea, especially in SDD-bearing eyes. Eyes with drusen also exhibited poor sensitivity but not as poor as SDD eyes and with similar but less severe regional effects.

The use of the ETDRS grid helped us to relate measures of visual function to the topography of photoreceptors, especially rods, and ultimately rod-driven neural circuitry.[12,44,45] Precise topographic analysis is a powerful tool for probing mechanisms underlying neurodegeneration, because the high dynamic range in human photoreceptor density provides a strong independent variable. Cone photoreceptor density peaks in the foveal central bouquet and decreases by 10-fold at 1 mm of eccentricity (approximately 3.5°).[12] Rods appear at approximately 175 µm from the central bouquet and increase to a maximum density similar to that of cones (approximately 150,000/ mm^2) in an elliptical ring at the arcades that surrounds the optic nerve head.[12] The inner slope of the rod ring (0.5–2.0 mm eccentricity) is proportionately more affected by cell loss in aging than the crest of the ring (2–5 mm eccentricity).[2] Similarly, our functional data, combined with others', suggest that scotopic sensitivity loss is proportionately greater in the central ETDRS subfield, where rods are sparse to begin with, versus the outer ring (Table 2 and Supplementary Table S3). A microperimetry test grid can standardize sensitivity assessment, but it does not eliminate selection bias in the choice of photoreceptors being assessed. All but the central four points in our MP1-S grid were rod dominated (Fig. 1). No test location probed only cones. In comparison with previous studies,[20,22,27,28,30] we tested scotopic sensitivity closer to the foveal center. Our data underscore the importance of small stimuli (Goldmann III 0.43°) even for rod-mediated vision[46] for which spatial summation is larger than for cones.[47] The larger Goldman V stimulus (1.72°),[20,22,25,28–31,48] centered at low eccentricities will access higher rod densities on the inner slope of the rod ring and thus may overestimate true sensitivity.

Like others,[24,25,28–30] we detected decrements in rod sensitivity in cone-dominated foveal areas with few rods with sensitivities that are low.[49] Studies using a coarse sampling grid in a modified standard perimeter were the first to identify that rod-mediated vision in eyes with AMD was reduced more in the central compared with the peripheral macula.[10,50] Initial microperimetry studies of eyes with SDD under mesopic conditions[18,19] suggested that mesopic dysfunction matched the areas of high SDD content. Using a dark-adapted chromatic perimeter, Fraser et al.[24] examined dark adaptation kinetics at 4°, 6°, and 12° on the inferior and superior retina, and at 12° nasal and temporal. Although they revealed that eyes with AMD and SDD exhibited more reduced static and dynamic rod function than eyes without SDD, they found that the greatest functional loss was within the central 6° of the retina. Using the same device, Flynn et al.[25] measured the scotopic thresholds in participants with AMD at 2°, 4°, 6°, 8°, 10°, 12°, and 18° eccentricity along the vertical retinal meridian, and confirmed that subjects with SDD had markedly elevated scotopic thresholds at the testing points of −4° to 8° compared with the

Investigative Ophthalmology & Visual Science

other testing loci. Tan et al.[28] assessed rod-mediated function using the same dark-adapted chromatic perimeter over a circular retinal area including testing points at 2°, 4°, 6°, 8°, 12°, 17°, and 24° eccentricity. They found that rod-mediated function within 8° was preferentially affected in eyes with AMD with SDD with the poorest sensitivity at 4°, regardless of the level of photo bleach. Nittala et al.[29] divided 32 MP-1S testing points into ETDRS-like rings and found decreased scotopic sensitivity relative to normal eyes without a central deficit (within 4°). Moreover they found that drusen volume and area were better correlated with scotopic sensitivity than with mesopic sensitivity. Other microperimetry studies reported mean sensitivities in the macula, but did not test for regional effects.[31,51] Our work extends prior work by testing for rod vision closer to the rod-free zone and quantifying the relative scotopic sensitivity loss in patients with AMD with and without SDD.

Our functional data can provide insights regarding the impact of SDD on vision. A histologic analysis of eyes with AMD shows that photoreceptors are shortened and deflected around deposits,[5,15,52] and overlying Müller glia are reactive.[53] It was initially proposed that SDD represent byproducts of intercellular trafficking that accumulate and become oxidized owing to low levels of outer retinal antioxidants.[37] In turn, proinflammatory accumulations were also thought to be cytotoxic owing to direct contact with photoreceptors. Several lines of evidence now counter that narrative. By histochemistry and high-resolution histology,[8,53,54] SDD are less lipid rich than drusen and, thus, may be a lesser source of peroxidizable lipids than drusen. Far fewer invading immune cells are found in the subretinal space of early to intermediate eyes with AMD with SDD[8,53] than in the sub-RPE–basal lamina space of eyes with drusen, suggesting a less inflammatory environment.[52,55–60] Last, type 3 neovascularization in AMD (of retinal origin) strongly associates with SDD,[61] yet preferentially develops in the ETDRS inner ring, that is, remote from SDD-dense areas in the outer ring and beyond.[62,63] A parsimonious hypothesis is that the distribution of type 3 neovascularization and poor rod-mediated vision demonstrated herein are related to the same spatially specific phenomena and are indicated by presence of SDD.

The location where the current study identified poor scotopic sensitivity is vulnerable to delayed RMDA, which represents the earliest and most persistent visual dysfunction in aging through intermediate AMD. An associated structural change for RMDA was recently identified by an agnostic, deep-learning-assisted image analysis of more than 1200 OCT volumes.[34] This analysis revealed that reflectivity changes on either side of the ellipsoid zone were associated with slower RMDA at 0.5 mm (1.7°) eccentricity and not at 2 mm eccentricity (6.9°), the two locations tested. These authors proposed that this effect is related to the remarkably high concentration of high-risk soft drusen in the central ETDRS subfield and inner ring.[64,65] This central focality in turn has been attributed to a combination of focused lipid trafficking attendant to delivering xanthophyll carotenoids to foveal cells and aging changes of Bruch's membrane and choriocapillaris that impede egress of unneeded lipids to the choroidal circulation,[65,66] resulting in subfoveal accumulation of lipid. Rods are highly affected by this barrier because they are dependent on the RPE–Bruch's membrane–choriocapillaris for retinoids and other essentials from circulation. Cones are also affected, but are more resilient than rods, because they are additionally sustained by Müller glia (for retinoids via the second visual cycle and xanthophyll carotenoids)[60,66,67] and the retinal circulation. Collectively, the vertical superimposition of these cellular interactions results in a center of foveal cone resilience surrounded by a ring of parafoveal rod vulnerability,[68] as shown here. The unifying feature of this model is vascular insufficiency owing to choriocapillaris degeneration,[69] choroidal thinning,[70–72] and possible problems with the systemic circulation.[73] The center-surround hypothesis is being tested in an ongoing prospective and well-powered observational study.[68]

The strengths of this study include well-characterized eyes with AMD of two prognostically important phenotypes, the inclusion of areas with few rods, the use of small stimuli, and graphical display of differences among study groups. Although the AMD–SDD group was older on average than the two other groups, statistical comparisons were performed with age-adjusted linear regression. The limitations of this study include the small number of participants overall, the cross-sectional design limiting inferences on causality, the under-representation of cone-only areas, and a subjective clinical assessment rather than a direct quantification of deposit burden. A lack of information about cone-mediated sensitivity, also reported to decrease in eyes with SDD,[23] can be addressed in future studies using two-color dark-adapted perimetry.[74] Future studies will also examine fixation stability rigorously. As noted,[39] the lack of a significant difference between normal and drusen patients may be related to ceiling effects. In our study, we found no testing points yielding a result of 30 dB (the ceiling light level) in the normal group. In the AMD–drusen group, mesopic sensitivity reached the "ceiling" at 3 (of 68) testing points in one subject's eye, whereas scotopic sensitivity reached the "ceiling" at 3 (of 68) testing points in another subject's eye. Thus, we decreased but could not completely eliminate the ceiling effect in our results. Despite these limitations, our data extend a previously noted spatial dissociation of SDD and greatest rod-mediated visual deficits and contribute important new information about the significance of SDD in AMD pathophysiology. Whether the distribution of SDD follows rods, spares the fovea, or both is a critical open question to be addressed in future research.

In conclusion, SDD have far-reaching impact in the central ETDRS subfield in eyes with AMD, indicating other factors in this region beyond the deposits themselves contribute to poor vision. Our findings should be confirmed in larger cohorts of patients with AMD.

Acknowledgments

Supported by NIH R01EY024378, R21EY027948, R01EY029595, R01AG04212, P30EY003039, W F Keck Foundation, the Carl Marshall Reeves & Mildred Almen Reeves foundation, Research to Prevent Blindness/Dr. H. James and Carole Free Catalyst Award for Innovative Research Approaches for AMD, Research to Prevent Blindness institutional funds, EyeSight Foundation of Alabama, and the Buck Trust of Alabama. The sponsors or funding organizations had no role in the design or conduct of this research.

Disclosure: **Y. Zhang,** None; **T.A. Swain,** None; **M.E. Clark,** None; **K.R. Slone,** None; **W. Warriner,** None; **C. Owsley,** None; **S.R. Sadda,** Allergan (F,C), Carl Zeiss Meditec (F), Genentech (F, C), Optos (F,C), Topcon (F), Amgen (C), Apellis (C), Iveric (C), Centervue (C), Roche (C), Heidelberg (C), 4DMT (C), Bayer (C), Regeneron (C), Novartis (C), Oxurion (C); **D. Sarraf**, Amgen (F, C), Bayer (C), Genentech (C, F), Iveric Bio (C), Novartis (C), Optovue (F, C), Heidelberg (F), Regeneron (F)

and Topcon V (F); **C.A. Curcio,** Genentech (F), Regeneron (F), MacRegen (I)

References

1. Spaide RF. Improving the age-related macular degeneration construct: a new classification system. *Retina.* 2018;38(5):891–899.
2. Curcio CA, Millican CL, Allen KA, Kalina RE. Aging of the human photoreceptor mosaic: evidence for selective vulnerability of rods in central retina. *Invest Ophthalmol Vis Sci.* 1993;34(12):3278–3296.
3. Curcio CA, Medeiros NE, Millican CL. Photoreceptor loss in age-related macular degeneration. *Invest Ophthalmol Vis Sci.* 1996;37(7):1236–1249.
4. Adler R, Curcio C, Hicks D, Price D, Wong F. Cell death in age-related macular degeneration. *Mol Vis.* 1999;5:31.
5. Curcio CA, Messinger JD, Sloan KR, McGwin G, Medeiros NE, Spaide RF. Subretinal drusenoid deposits in non-neovascular age-related macular degeneration: morphology, prevalence, topography, and biogenesis model. *Retina.* 2013;33(2):265–276.
6. Curcio CA. Soft drusen in age-related macular degeneration: biology and targeting via the oil spill strategies. *Invest Ophthalmol Vis Sci.* 2018;59(4):AMD160–AMD181.
7. Chen L, Messinger JD, Sloan KR, et al. Nonexudative macular neovascularization supporting outer retina in age-related macular degeneration: a clinicopathologic correlation. *Ophthalmology.* 2020;127(7):931–947.
8. Chen L, Messinger JD, Kar D, Duncan JL, Curcio CA. Biometrics, impact, and significance of basal linear deposit and subretinal drusenoid deposit in age-related macular degeneration. *Invest Ophthalmol Vis Sci.* 2021;62(1):33.
9. Curcio CA, Owsley C, Jackson GR. Spare the rods, save the cones in aging and age-related maculopathy. *Invest Ophthalmol Vis Sci.* 2000;41(8):2015–2018.
10. Owsley C, Jackson GR, Cideciyan AV, et al. Psychophysical evidence for rod vulnerability in age-related macular degeneration. *Invest Ophthalmol Vis Sci.* 2000;41(1):267–273.
11. Jackson GR, Owsley C, Curcio CA. Photoreceptor degeneration and dysfunction in aging and age-related maculopathy. *Ageing Res Rev.* 2002;1(3):381–396.
12. Curcio CA, Sloan KR, Kalina RE, Hendrickson AE. Human photoreceptor topography. *J Comp Neurol.* 1990;292(4):497–523.
13. Bringmann A, Syrbe S, Gorner K, et al. The primate fovea: structure, function and development. *Prog Retin Eye Res.* 2018;66:49–84.
14. Spaide RF, Ooto S, Curcio CA. Subretinal drusenoid deposits aka pseudodrusen. *Surv Ophthalmol.* 2018;63(6):782–815.
15. Chen L, Messinger JD, Zhang Y, Spaide RF, Freund KB, Curcio CA. Subretinal drusenoid deposit in age-related macular degeneration: histologic insights into initiation, progression to atrophy, and imaging. *Retina.* 2020;40(4):618–631.
16. Steinberg JS, Fleckenstein M, Holz FG, Schmitz-Valckenberg S. Foveal sparing of reticular drusen in eyes with early and intermediate age-related macular degeneration. *Invest Ophthalmol Vis Sci.* 2015;56(8):4267–4274.
17. Pfau M, Jolly JK, Wu Z, et al. Fundus-controlled perimetry (microperimetry): application as outcome measure in clinical trials. *Prog Retin Eye Res.* 2020;82:100907.
18. Ooto S, Ellabban AA, Ueda-Arakawa N, et al. Reduction of retinal sensitivity in eyes with reticular pseudodrusen. *Am J Ophthalmol.* 2013;156(6):1184–1191.e1182.
19. Querques G, Massamba N, Srour M, Boulanger E, Georges A, Souied EH. Impact of reticular pseudodrusen on macular function. *Retina.* 2014;34(2):321–329.
20. Steinberg JS, Fitzke FW, Fimmers R, Fleckenstein M, Holz FG, Schmitz-Valckenberg S. Scotopic and photopic microperimetry in patients with reticular drusen and age-related macular degeneration. *JAMA Ophthalmol.* 2015;133(6):690–697.
21. Flamendorf J, Agron E, Wong WT, et al. Impairments in dark adaptation are associated with age-related macular degeneration severity and reticular pseudodrusen. *Ophthalmology.* 2015;122(10):2053–2062.
22. Steinberg JS, Sassmannshausen M, Fleckenstein M, et al. Correlation of partial outer retinal thickness with scotopic and mesopic fundus-controlled perimetry in patients with reticular drusen. *Am J Ophthalmol.* 2016;168:52–61.
23. Wu Z, Ayton LN, Makeyeva G, Guymer RH, Luu CD. Impact of reticular pseudodrusen on microperimetry and multifocal electroretinography in intermediate age-related macular degeneration. *Invest Ophthalmol Vis Sci.* 2015;56(3):2100–2106.
24. Fraser RG, Tan R, Ayton LN, Caruso E, Guymer RH, Luu CD. Assessment of retinotopic rod photoreceptor function using a dark-adapted chromatic perimeter in intermediate age-related macular degeneration. *Invest Ophthalmol Vis Sci.* 2016;57(13):5436–5442.
25. Flynn OJ, Cukras CA, Jeffrey BG. Characterization of rod function phenotypes across a range of age-related macular degeneration severities and subretinal drusenoid deposits. *Invest Ophthalmol Vis Sci.* 2018;59(6):2411–2421.
26. Pfau M, Lindner M, Gliem M, et al. Mesopic and dark-adapted two-color fundus-controlled perimetry in patients with cuticular, reticular, and soft drusen. *Eye (Lond).* 2018;32(12):1819–1830.
27. Sassmannshausen M, Steinberg JS, Fimmers R, et al. Structure-function analysis in patients with intermediate age-related macular degeneration. *Invest Ophthalmol Vis Sci.* 2018;59(3):1599–1608.
28. Tan R, Guymer RH, Luu CD. Subretinal drusenoid deposits and the loss of rod function in intermediate age-related macular degeneration. *Invest Ophthalmol Vis Sci.* 2018;59(10):4154–4161.
29. Nittala MG, Velaga SB, Hariri A, et al. Retinal sensitivity using microperimetry in age-related macular degeneration in an Amish population. *Ophthalmic Surg Lasers Imaging Retina.* 2019;50(9):e236–e241.
30. Tan RS, Guymer RH, Aung KZ, Caruso E, Luu CD. Longitudinal assessment of rod function in intermediate age-related macular degeneration with and without reticular pseudodrusen. *Invest Ophthalmol Vis Sci.* 2019;60(5):1511–1518.
31. Corvi F, Pellegrini M, Belotti M, Bianchi C, Staurenghi G. Scotopic and fast mesopic microperimetry in eyes with drusen and reticular pseudodrusen. *Retina.* 2019;39(12):2378–2383.
32. Sassmannshausen M, Pfau M, Thiele S, et al. Longitudinal analysis of structural and functional changes in presence of reticular pseudodrusen associated with age-related macular degeneration. *Invest Ophthalmol Vis Sci.* 2020;61(10):19.
33. Curcio CA. Photoreceptor topography in ageing and age-related maculopathy. *Eye.* 2001;15(3):376–383.
34. Lee AY, Lee CS, Blazes MS, et al. Exploring a structural basis for delayed rod-mediated dark adaptation in age-related macular degeneration via deep learning. *Transl Vis Sci Technol.* 2020;9(2):62.
35. Davis MD, Gangnon RE, Lee LY, et al. The Age-Related Eye Disease Study severity scale for age-related macular degeneration: AREDS report no. 17. *Arch Ophthalmol.* 2005;123(11):1484–1498.
36. Zhang Y, Wang X, Rivero EB, et al. Photoreceptor perturbation around subretinal drusenoid deposits as revealed by adaptive optics scanning laser ophthalmoscopy. *Am J Ophthalmol.* 2014;158(3):584–596.e581.

Investigative Ophthalmology & Visual Science

37. Zweifel SA, Spaide RF, Curcio CA, Malek G, Imamura Y. Reticular pseudodrusen are subretinal drusenoid deposits. *Ophthalmology.* 2010;117(2):303–312. e301.
38. Spaide RF, Curcio CA. Drusen characterization with multimodal imaging. *Retina.* 2010;30(9):1441–1454.
39. Acton JH, Bartlett NS, Greenstein VC. Comparing the Nidek MP-1 and Humphrey field analyzer in normal subjects. *Optom Vis Sci.* 2011;88(11):1288–1297.
40. Cassels NK, Wild JM, Margrain TH, Chong V, Acton JH. The use of microperimetry in assessing visual function in age-related macular degeneration. *Surv Ophthalmol.* 2018;63(1):40–55.
41. Kleefeldt N, Bermond K, Tarau IS, et al. Quantitative fundus autofluorescence: advanced analysis tools. *Transl Vis Sci Technol.* 2020;9(8):2.
42. Crameri F, Shephard GE, Heron PJ. The misuse of colour in science communication. *Nat Commun.* 2020;11(1):5444.
43. Klein R, Davis MD, Magli YL, Segal P, Klein BE, Hubbard L. The Wisconsin Age-Related Maculopathy Grading System. *Ophthalmology.* 1991;98(7):1128–1134.
44. Lee SCS, Martin PR, Grunert U. Topography of neurons in the rod pathway of human retina. *Invest Ophthalmol Vis Sci.* 2019;60(8):2848–2859.
45. Wilkinson MO, Anderson RS, Bradley A, Thibos LN. Resolution acuity across the visual field for mesopic and scotopic illumination. *J Vis.* 2020;20(10):7.
46. Sharpe LT, Stockman A, Fach CC, Markstahler U. Temporal and spatial summation in the human rod visual system. *J Physiol.* 1993;463:325–348.
47. Volbrecht VJ, Shrago EE, Schefrin BE, Werner JS. Spatial summation in human cone mechanisms from 0 degrees to 20 degrees in the superior retina. *J Opt Soc Am A Opt Image Sci Vis.* 2000;17(3):641–650.
48. Steinberg JS, Sassmannshausen M, Pfau M, et al. Evaluation of two systems for fundus-controlled scotopic and mesopic perimetry in eye with age-related macular degeneration. *Transl Vis Sci Technol.* 2017;6(4):7.
49. Massof RW, Finkelstein D. Rod sensitivity relative to cone sensitivity in retinitis pigmentosa. *Invest Ophthalmol Vis Sci.* 1979;18(3):263–272.
50. Steinmetz RL, Haimovici R, Jubb C, Fitzke FW, Bird AC. Symptomatic abnormalities of dark adaptation in patients with age-related Bruch's membrane change. *Br J Ophthalmol.* 1993;77(9):549–554.
51. Nassisi M, Tepelus T, Corradetti G, Sadda SR. Relationship between choriocapillaris flow and scotopic microperimetry in early and intermediate age-related macular degeneration. *Am J Ophthalmol.* 2021;222:302–309.
52. Sarks JP, Sarks SH, Killingsworth MC. Evolution of geographic atrophy of the retinal pigment epithelium. *Eye (Lond).* 1988;2(Pt 5):552–577.
53. Greferath U, Guymer RH, Vessey KA, Brassington K, Fletcher EL. Correlation of histologic features with in vivo imaging of reticular pseudodrusen. *Ophthalmology.* 2016;123(6):1320–1331.
54. Oak AS, Messinger JD, Curcio CA. Subretinal drusenoid deposits: further characterization by lipid histochemistry. *Retina.* 2014;34(4):825–826.
55. Penfold PL, Killingsworth MC, Sarks SH. Senile macular degeneration. The involvement of giant cells in atrophy of the retinal pigment epithelium. *Invest Ophthalmol Vis Sci.* 1986;27(3):364–371.
56. Zanzottera EC, Messinger JD, Ach T, Smith RT, Curcio CA. Subducted and melanotic cells in advanced age-related macular degeneration are derived from retinal pigment epithelium. *Invest Ophthalmol Vis Sci.* 2015;56(5):3269–3278.
57. McLeod DS, Bhutto I, Edwards MM, Silver RE, Seddon JM, Lutty GA. Distribution and quantification of choroidal macrophages in human eyes with age-related macular degeneration. *Invest Ophthalmol Vis Sci.* 2016;57(14):5843–5855.
58. Zanzottera EC, Ach T, Huisingh C, Messinger JD, Spaide RF, Curcio CA. Visualizing retinal pigment epithelium phenotypes in the transition to geographic atrophy in age-related macular degeneration. *Retina.* 2016;36(Suppl 1):S12–S25.
59. Li M, Dolz-Marco R, Huisingh C, et al. Clinicopathologic correlation of geographic atrophy secondary to age-related macular degeneration. *Retina.* 2019;39(4):802–816.
60. Cao D, Leong B, Messinger JD, et al. Hyperreflective foci, optical coherence tomography progression indicators in age-related macular degeneration, include transdifferentiated retinal pigment epithelium. *Invest Ophthalmol Vis Sci.* 2021;62(10):34.
61. Spaide RF, Jaffe GJ, Sarraf D, et al. Consensus nomenclature for reporting neovascular age-related macular degeneration data: consensus on neovascular age-related macular degeneration nomenclature study group. *Ophthalmology.* 2020;127(5):616–636.
62. Haj Najeeb B, Deak G, Schmidt-Erfurth U, Gerendas BS. The RAP study, report two: the regional distribution of macular neovascularization type 3, a novel insight into its etiology. *Retina.* 2020;40(10):1980–1987.
63. Kim JH, Chang YS, Kim JW, Kim CG, Lee DW. Characteristics of type 3 neovascularization lesions: focus on the incidence of multifocal lesions and the distribution of lesion location. *Retina.* 2020;40(6):1124–1131.
64. Wang Q, Chappell RJ, Klein R, et al. Pattern of age-related maculopathy in the macular area. The Beaver Dam Eye Study. *Invest Ophthalmol Vis Sci.* 1996;37(11):2234–2242.
65. Pollreisz A, Reiter GS, Bogunovic H, et al. Topographic distribution and progression of soft drusen volume in age-related macular degeneration implicate neurobiology of fovea. *Invest Ophthalmol Vis Sci.* 2021;62(2):26–26.
66. Curcio CA. Antecedents of soft drusen, the specific deposits of age-related macular degeneration, in the biology of human macula. *Invest Ophthalmol Vis Sci.* 2018;59(4):Amd182–amd194.
67. Wang JS, Kefalov VJ. The cone-specific visual cycle. *Prog Retin Eye Res.* 2011;30(2):115–128.
68. Curcio CA, McGwin G, Jr., Sadda SR, et al. Functionally validated imaging endpoints in the Alabama Study on Early Age-related Macular Degeneration 2 (ALSTAR2): Design and methods. *BMC Ophthalmol.* 2020;20(1):196.
69. Lutty GA, McLeod DS, Bhutto IA, Edwards MM, Seddon JM. Choriocapillaris dropout in early age-related macular degeneration. *Exp Eye Res.* 2020;192:107939.
70. Querques G, Querques L, Forte R, Massamba N, Coscas F, Souied EH. Choroidal changes associated with reticular pseudodrusen. *Invest Ophthalmol Vis Sci.* 2012;53(3):1258–1263.
71. Switzer DW, Jr., Mendonça LS, Saito M, Zweifel SA, Spaide RF. Segregation of ophthalmoscopic characteristics according to choroidal thickness in patients with early age-related macular degeneration. *Retina.* 2012;32(7):1265–1271.
72. Garg A, Oll M, Yzer S, et al. Reticular pseudodrusen in early age-related macular degeneration are associated with choroidal thinning. *Invest Ophthalmol Vis Sci.* 2013;54(10):7075–7081.
73. Rastogi N, Smith RT. Association of age-related macular degeneration and reticular macular disease with cardiovascular disease. *Surv Ophthalmol.* 2016;61(4):422–433.
74. Pfau M, Lindner M, Muller PL, et al. Effective dynamic range and retest reliability of dark-adapted two-color fundus-controlled perimetry in patients with macular diseases. *Invest Ophthalmol Vis Sci.* 2017;58(6):BIO158–BIO167.

Investigative Ophthalmology & Visual Science